Failure models for composite structures under compression loading

Conference Paper · October 2011

CITATIONS
0

READS
1,323

3 authors, including:

Marcelo Leite Ribeiro
University of São Paulo
147 PUBLICATIONS **931** CITATIONS
SEE PROFILE

Volnei Tita
University of São Paulo
309 PUBLICATIONS **2,760** CITATIONS
SEE PROFILE

Failure models for composite structures under compression loading

Marcelo Leite Ribeiro, strova@hotmail.com
Volnei Tita, voltita@sc.usp.br
Department of Aeronautical Engineering - Engineering School of São Carlos, University of São Paulo, São Carlos, SP, Brazil

Dirk Vandepitte, dirk.vandepitte@mech.kuleuven.be
Production Engineering, Machine Design and Automation (PMA) Section, Katholiek Universiteit Leuven, Leuven, Belgium

Abstract. *The increase in the use of composite materials in primary structures makes the understanding of structural behaviour an important issue. The correct prediction of failure and the damage evolution allows for the development of more efficient structures. While under tensile loads most of composite structures present an elastic brittle behaviour, under compression a non-linear elastic and brittle behaviour can be observed. This work presents a study of failure of composite structures under compression loads, as well as the progressive damage analysis of these structures until their complete collapse. The failure model was implemented as Fortran subroutine, which is linked to finite element software, ABAQUS^{TM}, in order to predict the composite structures behaviour. Experimental tests were performed to identify the material model parameters as well as to verify the proposed model. The numerical model perform well in simulate the composite failure process under compression loads.*

Keywords: *composite materials, compression loads, numerical models, progressive damage analysis.*

1. Introduction

In the last years, the use of composite materials as a primary structural element has been increasing. Some new aircraft designs, such as Airbus A380 and Boeing 787 use composite materials even for primary structural elements such as wing spars and fuselage skins, achieving lighter structures without loss of airworthiness. However, the application of composite in structures is still limited by the difficulty in predicting their service life (Travessa, 2006). From the designer standpoint, having failure criteria which predicts, with a reasonable accuracy, the damage process in lamina to structural level is essential to help the design process.

Although the increasing number of failure criteria and progressive failure models, the failure process and subsequent damage evolution is still underdeveloped. Also, the difficulty in predicting the structural failure modes results in the need for a well planned test program (Maimí *et al.*, 2007).

However, the compression behaviour of composite laminates is very complex, due to many concurrent phenomena during composite laminate failure under compression load. Fiber micro-buckling, splitting and shear band (Yokozeki *et al.*, 2005) are some effects which should be considered when a structure made from composite material is subjected by compression loads. Also, compression failure still a design limiting factor for aligned, continuous long fibers composites, in which the compressive strength is often lower than 60% of tensile strength (Budiansky and Fleck, 1993).

This work, presents a study of failure of composite structures under compression loads, as well as the progressive damage analysis of these structures until their complete collapse. Starting from Ladevèze and LeDantec (1992) and Allix *et al.* (1994) work, the present work introduces some modifications improving this model.

2. Failure Mechanisms

Due to composite materials heterogeneity, typically these materials exhibit multiple damage before the total lamina rupture. This behaviour makes failure of composite materials and structures very complex and not well defined. The failure process involves a different number of failure mechanism, such as fiber fracture, fiber pull out, matrix cracking, fiber/matrix debonds, fiber kinking and radial Interface cracks and fiber splitting. When the fibers are the primary load carrying component the most critical failure mechanism is the transverse fiber fracture, which leads to a rupture of a continuous fiber into two or more distinct segments (Herakovich, 1998). Composite laminates made from the stacking of plies, which contains a polymeric matrix reinforced by fibers, shows two types of failure modes. Intra-ply failure modes which is characterized by damage at fibers, polymeric matrix and/or interface between fibers and matrix (Fig.1(a)). The intra-ply failure mechanism are: 1 fiber pill-out, 2 fiber bridging, 3 fiber and matrix debonding, 4 fiber rupture and mechanism 5 matrix cracks (Tita, 2003).

1. Intra-ply failure modes: damage at fibers, polymeric matrix and/or interface between fibers and matrix (Fig.1(a));
2. Inter-ply failure modes: delaminations between plies (Fig.1(b)).

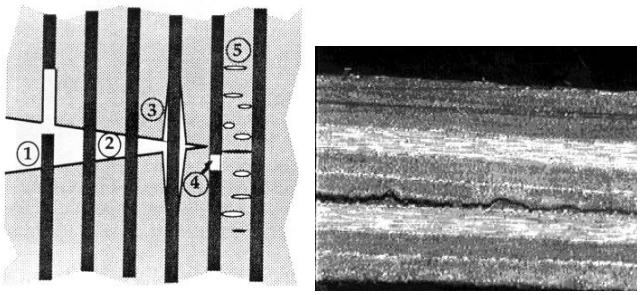

(a) (b)

Figure 1. ((a) intra-ply failure of composite Anderson (1995) ; (b) inter-ply failure of composite (delamination).

The inter-ply failure, called delamination (Fig.1(b)), occurs after intra-ply damages, i.e., the evolution of intra-ply damages lead to the delaminations, because the damaged regions grow when the load increases. Also the cracks at two adjacent plies (with different orientation angle) join for creating a discrete failure between these layers. At that moment, the interlaminar shear increases strongly and the delamination process initiates. This failure mechanism is very common to occur under flexural and transversal shear stresses due to quasi-static or dynamic loading. Material models for intra-ply damages have been improved, and some material models for delamination have been developed (Tita, 2003).

Under compression loads, laminate failure mostly occurs due to elastic instability of the fibers (Puck and Schürmann, 1998). However, the compression failure mechanism is more complex and, depending on the material, different compressive failure modes are possible: Microbuckling, Kinking and Fiber Failure (Pinho, 2005).

The most popular numerical technique for structural analysis is the finite element method, this method allows modeling complex structures and their failure. It may not be a simple task, mostly when a progressive failure analysis is performed. Some models demand a high computational effort and the analysis time may be considerable. Also, material that presents softening behaviour and stiffness degradation normally presents severe convergence problems, mostly when using implicit finite elements programs (Lapczyk and Hurtado, 2007). Nevertheless computational simulations can reduce the characterization costs of composite materials, also can support the optimization of these materials (Van Der Meer and Sluys, 2009).

In order to perform a progressive failure analysis, the first ply failure must be captured. For this task, there are a number of failure theories available in the current literature. Due to simplicity of use, the early theories, for example, Tsai-Wu, maximum stress, maximum strain and Hashin are still applied in analysis of laminate (Tay *et al.*, 2008) in order to capture the initial failure.

2.1 Longitudinal Failure

When a unidirectional composite lamina is loaded in fiber direction (see Fig.2(a)), the largest portion of the load is supported by the fibers due to their high stiffness compared to the matrix, also the transmission of tensile loads in the fibers is not impacted by the state of damage in the matrix (Matzenmiller *et al.*, 1995). The behaviour of unidirectional lamina varies with several factors such as fiber volume fraction, matrix material, fiber material, manufacturing process, compressive or tensile load, etc. After fiber failure, the internal loads are redistributed to other areas, and it may cause a structural collapse (Maimí *et al.*, 2007).

In UD composites, intralaminar failure mechanisms trigger structural collapse almost immediately, however multidirectional composites can support an increase of intralaminar failure before collapse (Maimí *et al.*, 2007).

Under compressive load in fiber direction, the composite failure is considered to be a microbuckling problem. This phenomenon is influenced by several factors such as fiber size and shape, fiber waviness, fiber matrix bonding, fiber and matrix stiffness and fiber and matrix compressive strength (Herakovich, 1998). The compressive load carrying capacity is severely affect by the effective stiffness and strength of matrix phase. The matrix works as an elastic base for the fibers under compression (Matzenmiller *et al.*, 1995).

Also compressive strength of composite materials is highly dependent on the fiber alignment, which low values of misalignment can lead to a drastic reduction on the compression strength (Wisnom, 1990).

2.2 Transverse Failure

The transverse behaviour of unidirectional composite materials is highly anisotropic and, low strength in the transverse direction. Even when loaded in fiber direction the composite could fail in transverse direction with several factors having a significant influence on the transverse strength (Callister, 2001).

In the transverse direction, the normal and shear stresses are transmitted by both matrix and fibers. But the damage occurs in the matrix and in the fiber matrix interface. Usually, the bond strength between fiber and matrix are lower than

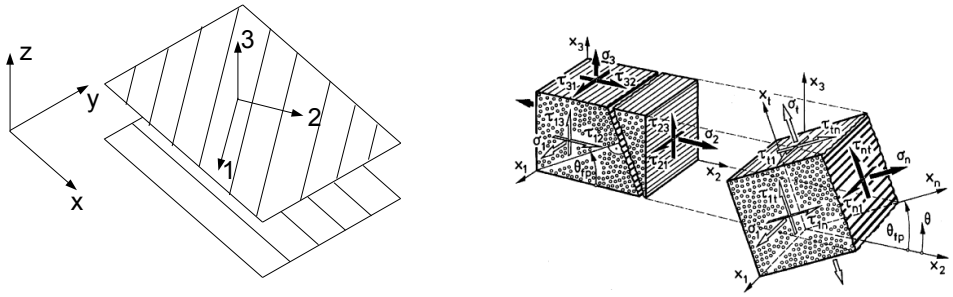

(a) (b)

Figure 2. (a)Lamina coordinate system, (b) Failure plane orientation, ((Puck and Schürmann, 2002)).

the strength of each single constituent (Matzenmiller *et al.*, 1995).

Under transverse tensile loading, $\sigma_{22} > 0$ and in-plane shear stress τ_{12}, the existing defects presents in a ply (small debonds, voids, resin rich regions) trigger a transverse crack that extends through the ply thickness (Maimí *et al.*, 2007). These defects produce a non-linear behaviour in the relation between shear stress τ_{12} and shear strain γ_{12} before the failure. This non-linear behaviour is also due to visco-plastic behaviour of the matrix (Puck and Schürmann, 2002). These transverse cracks do not produce any effect in the fibers.

Under transverse compressive load, $\sigma_{22} < 0$, matrix cracks crush in the sense of "fragmentation" of brittle matrix materials (Matzenmiller *et al.*, 1995). If the normal stress acting in the failure plane is compressive, $\sigma_n < 0$, the failure is due to failure plane shear stresses, τ_{nl} and τ_{nt}, in this case σ_n prevents the shear fracture (Puck and Schürmann, 2002). Figure2(b) shows the notations and coordinate system for unidirectional composite.

Another important feature of composite failure in transverse direction is how the shear stress affects the failure plane angle. Under a high value of in-plane shear stress when compared with transverse stress ($\tau_{12} > \sigma_{22}$), the fracture plane is perpendicular to the mid-plane. Increasing σ_{22}, the fracture plane angle changes (Maimí *et al.*, 2007).

3. MATERIAL MODEL

In order to model the behaviour of composite structures, a new material model is proposed, which has the following objectives:

- Be simple to be implemented;
- Possess low computational cost;
- Need only simple tests for model parameters determination;
- Need only simple tests coupons to be manufactured.

In order to achieve these objectives, during the bibliographical revision some models were studied more deeply. A model presented by Ladevèze and LeDantec (1992) and Allix *et al.* (1994), who use a damage mechanics approach and thermodynamic forces to model the progressive failure of the composite structures. This model works as a starting point for the present work.

This model is capable to distinguish between two ply degradation mechanisms (matrix micro-cracking and fiber matrix debonding). Plane stress state are assumed (Herakovich, 1998). Matrix is considered to be isotropic and possess an isotropic hardening behaviour with associative plastic surface evolution in σ_{22} x τ_{12} plane.

To capture the failure in fiber direction, Ladevèze and LeDantec (1992) and Allix *et al.* (1994) use the simple maximum stress failure criteria, but for matrix the model assume uses classical plasticity theory and the damage onset occurs when the elastic domain function f is equal to zero (see Fig.3(a)).

Some considerations about the model damage parameters are summarized in Table 1.

The thermodynamic forces (Y_1, Y_2 and Y_6) associated with internal damage variables, d_i, $i = 1, 2, 6$, are related to the strain energy density E_D as are show in eq. 1 (Herakovich, 1998).

$$Y_1 = \frac{\partial E_D}{\partial d_1}, Y_2 = \frac{\partial E_D}{\partial d_2}, Y_6 = \frac{\partial E_D}{\partial d_6} \tag{1}$$

Table 1. Model hypothesis for fiber and matrix. Allix *et al.* (1994) and Ladevèze and LeDantec (1992).

Damage Parameter	**Tensile**	**Compression**
d_1	Linear elastic brittle behaviour, $d_1 = 0$ or $d_1 = 1$	Non-linear elastic behaviour. The elastic modulus decrease as follows $E_{11} = E_{11}^0 + \alpha\epsilon_{11}$
d_2	Linear damage evolution	No damage evolution
d_6	Linear damage evolution	Linear damage evolution

The damaged strain energy is show in eq.2:

$$E_D = \frac{1}{2}\left[\frac{\sigma_{11}^2}{E_{11}^0(1-d_1)} - 2\frac{\nu_{12}^0}{E_{11}^0}\sigma_{11}\sigma_{22} + \frac{\langle\sigma_{22}^2\rangle_+}{E_{22}^0(1-d_2)} + \frac{\langle\sigma_{22}^2\rangle_-}{E_{22}^0} + \frac{\sigma_{12}^2}{G_{12}^0(1-d_6)}\right] \tag{2}$$

The model parameters, material properties and strength can be obtained easily by simple experimental tests. In order to measure the stiffness degradation cyclic tests need to be performed, (Ladevèze and LeDantec, 1992).

Some experimental tests are standard test but others are non-standard test, for example a tensile cyclic test in a cross-ply $\pm 67.5^o$ laminates, which is necessary in order to measure the coupling between shear stress, τ_{12}, and transverse stress, σ_{22}, once this test leads to a bi-axial stress state. The coupling relation appears in eq.3 by parameter b and in eq.4 by parameter a.

$$Y = \sqrt{Y_6 + bY_2} \tag{3}$$

Shear stress τ_{12}, and transverse stress σ_{22}, play a role in the matrix damage process. Also a plastic surface in the τ_{12} x σ_{22} plane with isotropic hardening model is adopted to model the failure. The evolution of the elastic domain for matrix is considered to be associative, see Fig.3(b). The elastic domain function is presented in eq.4.

$$f = \sqrt{\tilde{\tau_{12}}^2 + a^2\tilde{\sigma_{22}}^2} - (R(\tilde{p}) + R_0) \tag{4}$$

Where $\tilde{\tau_{12}}$ is the effective shear stress and $\tilde{\sigma_{22}}$ is the effective transverse stress (see eq.5).

$$\tilde{\tau_{12}} = \frac{\tau_{12}}{(1-d_6)}, \tilde{\sigma_{22}} = \frac{\sigma_{22}}{(1-d_2)} \tag{5}$$

Allix *et al.* (1994) propose a new experimental test set-up to measure the composite properties under compression loads. The behaviour of unidirectional lamina under compression can be regarded as non-linear elastic and this behaviour was modeled using a secant modulus. The damage evolution d_2 and d_6, due to σ_{22} and τ_{12} respectively, was assumed to be linear as shown in Fig.3(a).

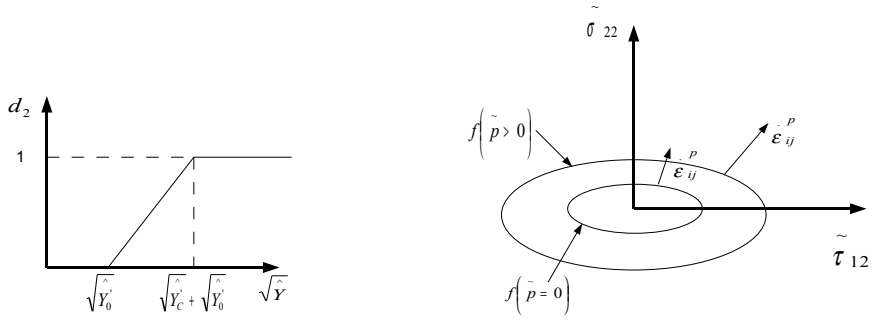

(a) (b)

Figure 3. (a)Linear damage evolution law, (b)Plastic surface evolution.

In other to account for the coupling of σ_{22} and τ_{12} in the plastic surface, the cumulative plastic strain, $\tilde{p}$, another parameter, a can be obtained from the $\pm 67.5^o$ cyclic tensile test as shown in eq.6.

$$\tilde{p} = \int_0^t \sqrt{4\left(\tilde{\epsilon_{12}}^p\right)^2 + \frac{1}{a^2}\left(\tilde{\epsilon_{22}}^p\right)^2}dt \tag{6}$$

In order to avoid the material healing, which is thermodynamically inconsistent, the thermodynamic force Y (eq.3) is the maximum value for all previous time up to the present time (Herakovich, 1998). The same consideration is made for the damage parameters d_2 and d_6.

The present work, is based on the same considerations as were stated before. It further introduces some modifications improving Ladevèze and LeDantec (1992) and Allix *et al.* (1994) model, one of these modifications is to include the effect of damage in the ν_{12} and ν_{21} coefficients as shown in eq.7 used by Matzenmiller *et al.* (1995).

$$D = \frac{1}{K} \cdot \begin{bmatrix} (1-d_1)E_{11} & (1-d_1)(1-d_2)\nu_{21}E_{22} & 0 \\ (1-d_1)(1-d_2)\nu_{12}E_{11} & (1-d_2)E_{22} & 0 \\ 0 & 0 & K(1-d_6)G_{12} \end{bmatrix} \tag{7}$$

where $K = (1-(1-d_1)(1-d_2)\nu_{12}\nu_{21})$.

Also, the present model includes some other post-failure considerations for fiber under tensile and compressive loads. These considerations and the material model are show in Tab.2. Note that for compression E_{22} and G_{12} are not influenced by fiber degradation, but after the fiber failure, E_{22} and G_{12} are degraded to zero. For tensile conditions, the fiber failure do not affect E_{22} and G_{12} even after fiber failure (Tab.2)

Table 2. Model hypothesis for fiber and matrix. Allix *et al.* (1994) and Ladevèze and LeDantec (1992).

Failure Criteria	**Type of Failure**	**Degradation Law**
$\frac{\sigma_{11}}{X_T} \geq 1$	Fiber Tensile	$E_{11} = 0$
$\frac{\lvert\sigma_{11}\rvert}{X_C} \geq 1$	Fiber compression	$E_{11} = E_{11}^0 + \alpha\epsilon$, after compression limit: $E_{11} = E_{22} = G_{12} = 0$
$f \geq 0$	Matrix Tensile	$E_{22} = E_{22}^0\,(1-d_2)$; $d_2 = \frac{\left\langle \sqrt{\widehat{Y}} - \sqrt{\widehat{Y_0'}} \right\rangle_+}{\sqrt{\widehat{Y_c'}}}$
-	Matrix Compression	$E_{22} = E_{22}^0$
$f \geq 0$	Shear	$G_{12} = E_{12}^0\,(1-d_6)$; $d_6 = \frac{\left\langle \sqrt{\widehat{Y}} - \sqrt{\widehat{Y_0}} \right\rangle}{\sqrt{\widehat{Y_c}}}$

4. FINITE ELEMENT MODEL

A finite element model for compressive simulations were performed using commercial software ABAQUS™following the prescriptions of $ASTM3410$. The finite element model uses a first order hexahedron element with 8 nodes (C3D8) for end tabs and a first order 4 node shell element (S4) for composite coupon. The mesh is show in Fig.4.

The tab dimensions are 50.0mm x 25.0mm x 2.0mm, the coupon dimensions are 150.0mm x 25.0mm x 2.0mm. The finite element model dimensions are presented in Fig.4. All degrees of freedom of one pair of tabs are constrained (see the left tabs in Fig.4), on the other side, all degrees of freedom are constrained except u_x displacement (see Fig.4) a displacement in the negative x direction is imposed here (compression). These boundary conditions were choose in order to simulate the compression test for $[15^o]_{10}$ and $[30^o]_{10}$.

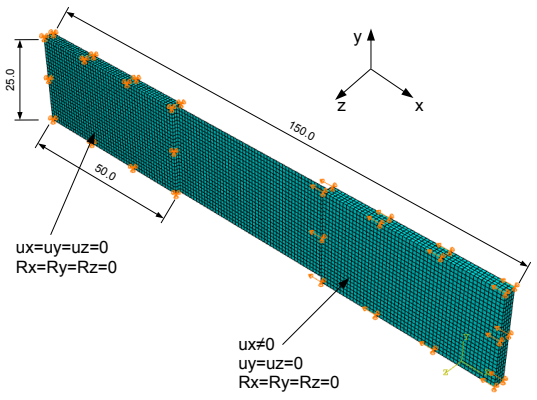

Figure 4. Finite element model, boundary conditions and mesh.

Tabs are regarded to be linear elastic and isotropic material (steel) and the coupon is modeled as a composite using a user material subroutine (UMAT) programmed as a FORTRAN subroutine which is linked to ABAQUS™. Tie constraint, which make all degrees of freedom the same for a pair of surfaces, is used in order to join together the tabs and the coupon.

5. EXPERIMENTAL TESTS

In order to obtain the model parameters, material elastic properties, strength values and also to validate the model, some experimental tests were performed. Table 3 shows which properties can be obtained from respective experimental test. Note that the $\pm 67.5^o$ is a non-standard test but the dimension for the test coupons are the same used for 90^0 coupons for tensile test.

Table 3. Experimental tests for model parameters and material characterization.

Test	**Standard**	**Dimensions** (mm)	**Properties**
Tensile 0^o	ASTM D3039	250.0 x 15.0 x 1.0	E_{11}, ν_{12}, X_T
Tensile 90^o	ASTM D3039	175.0 x 25.0 x 2.0	E_{22}, Y_T
Tensile $\pm 67.5^o$	N.A.	175.0 x 25.0 x 2.0	b, a, d_2
In-plane Shear $\pm 45^o$	ASTM D3518	250.0 x 25.0 x 2.7	G_{12}, S_{12}, d_6, $R + R_0$
Compression 0^o	ASTM D3410	150.0 x 10.0 x 2.0	α, X_C
Compression 90^o	ASTM D3410	150.0 x 25.0 x 2.0	Y_C

Tabs where used only for tensile experimental tests. After material characterization, some experimental tests were performed in order to evaluate the proposed model. These tests are shown in Table 4. The dimensions for this tests coupons were the same as used for 90^0 standard compression test.

Table 4. Experimental tests for model validation

Test	**Dimensions** (mm)
Compression Off-Axis 30^o	150.0 x 25.0 x 2.0
Compression Off-Axis 15^o	150.0 x 25.0 x 2.0

All coupons had a unidirectional (UD) structure with carbon fiber reinforcement, and coupons were manufactured by filament winding process. It is important to mention that the material properties, strength values as well as manufacture process will be not described as it is classified data.

The dimensions of the coupons follow the standards for each test performed even for off-axis coupons $[15^o]_{10}$ and $[30^o]_{10}$ as well as for cross-ply $[\pm 67.5^o]_{10}$ coupons.

Figure 5(a) shows the device for compression test and the image correlation camera. Figure 5(b) shows the $[0^o]_{10}$ coupon for compression test.

Some of the tensile tests for material characterization ($[0^o]_{10}$ and $[90^o]_{10}$) were performed at EESC/USP material engineering laboratory. The cross-ply $[\pm 67.5^o]_{10}$ tensile test were performed at KULeuven-MTM laboratory and all the compression tests were performed at KULeuven-MTM laboratory (see Fig.5(a)).

At USP an Emic test machine was used and for data acquisition strain gages and image correlation were used. At KULeuven an Instron universal test machine is used for compression tests, for data acquisition strain-gages were used in one test coupon face and digital image correlation in another face. A LIMESS system with VIC2D software was used for the digital image correlation analysis. On the other hand, at USP, the image correlation equipment consists of a Canon camera and a software programm in Matlab™was used. At both places, the force x displacement data were provided by the test machines.

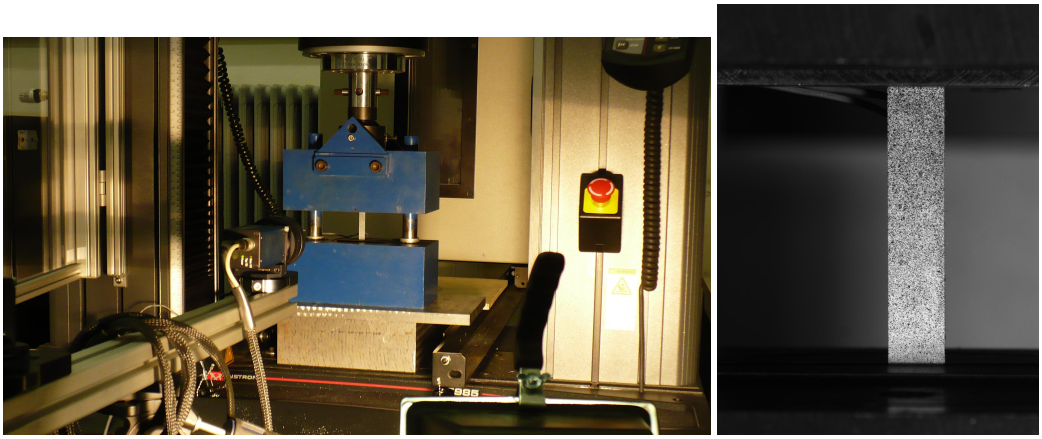

(a) (b)

Figure 5. (a)Compression test setup and data acquisition system (LUMISS and strain gages), (b) $[0^o]_{10}$ coupon for compression test.

A test speed of $0.5mm/min$ was applied for all compression experimental tests, both for loading or unloading cycles. In order to avoid low cycle fatigue the number of cycles is limited to a maximum of 5 (Allix *et al.*, 1994). For each test coupon orientation, a monotonic test was performed first in order to allow programming the load levels (upper and lower limits) for each loading and unloading cycle for that specific orientation.

6. RESULTS AND DISCUSSIONS

In order to evaluate the proposed material model, this model must be capable to simulate the behaviour of composite structures regardless of the degree of anisotropy. To accomplish this task, the results of the computational model were compared with $[15^o]_{10}$ and $[30^o]_{10}$ off-axis coupons used for compression test. Notice that those specific orientations were not used to calibrate the model.

Regarding the compression tests, some difficulties where founded during the tests. For some 0^o coupons where observed some brooming but no buckling. For 90^o and 30^o coupons buckling were the major problem during tests, mostly for 30^o. No problems where founded for 15^o coupons.

The experimental test results and the comparison between computational results with the experimental results for σ_{xx} x ϵ_{xx}, are shown in Fig.6(a) and (b) respectively. It is possible to observe that the model perform well to simulate the material response under compression loads for off-axis $[15^o]_{10}$.

Figure7(a) shows the $[15^o]_{10}$ after failure and Fig.7(b) shows the FEM model superposed the test coupon showing the correspondence between numerical model and experimental test.

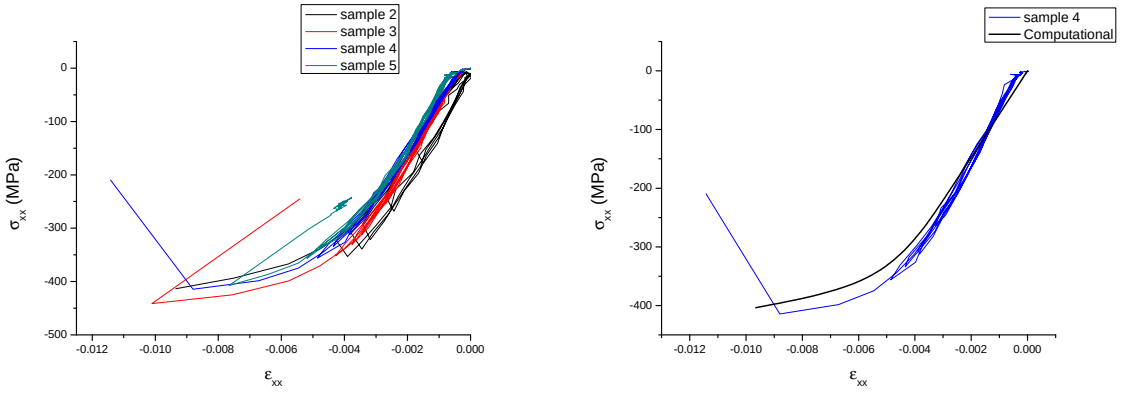

(a) (b)

Figure 6. (a) σ_{xx} x ϵ_{xx} Off-axis $[15^o]_{10}$ experimental tests results , (b) Off-axis $[15^o]_{10}$ σ_{xx} x ϵ_{xx} comparison between numerical and experimental

For off-axis $[30^o]_{10}$, the experimental tests results and computational results compared with the experimental results for σ_{xx} x ϵ_{xx} are shown in Fig.8(a) and (b) respectively. It is observed that the model performs well to simulate the material response under compression loads until failure, but after failure the computational value for σ_{xx} decreases while

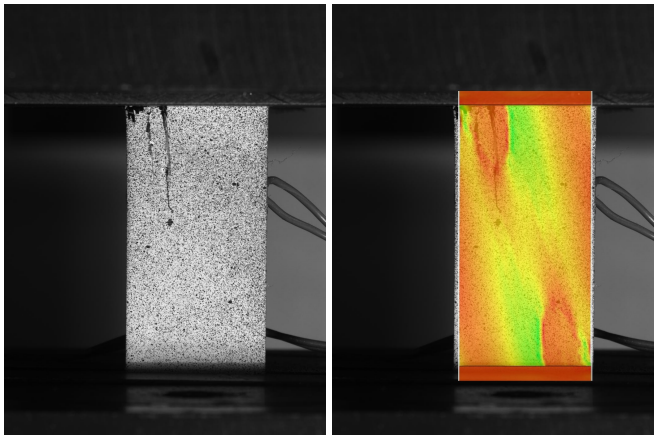

(a) (b)

Figure 7. (a)$[15^o]_{10}$ Off-Axis compression test coupon failure, (b)$[15^o]_{10}$ FEM model x Experimental test final failure.

the experimental results form a flat region.

It is important to mention that the compression test for off-axis $[30^o]_{10}$ did not fail only due to compressive loads but buckling was detected for all tested coupons mostly in the end of the test (relatively high loads). On the other hand, for off-axis $[15^o]$,$_{10}$ coupon, buckling was not detected until close to the failure. Buckling in the experiment could explain part of the differences after failure for $[30^o]_{10}$ off-axis coupons. Also, as for 30^o matrix modes are dominant in failure process, the softening in G_{12} due to d_6 ($d_2 = 0$ for $\sigma_{22} \leq 0$) does not lead to a brittle behaviour at failure. Nevertheless, the model behaves in a conservative way once the post-failure loads are lower than actual.

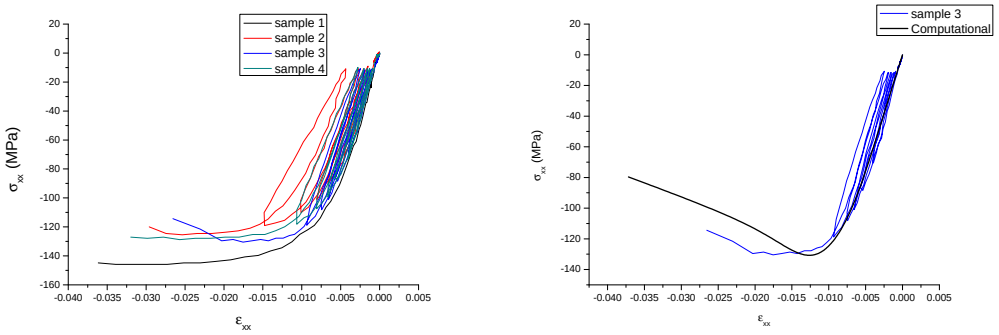

(a) (b)

Figure 8. (a) σ_{xx} x ϵ_{xx} Off-axis $[30^o]_{10}$ experimental test results , (b) Off-axis $[30^o]_{10}$ σ_{xx} x ϵ_{xx} comparison between numerical and experimental.

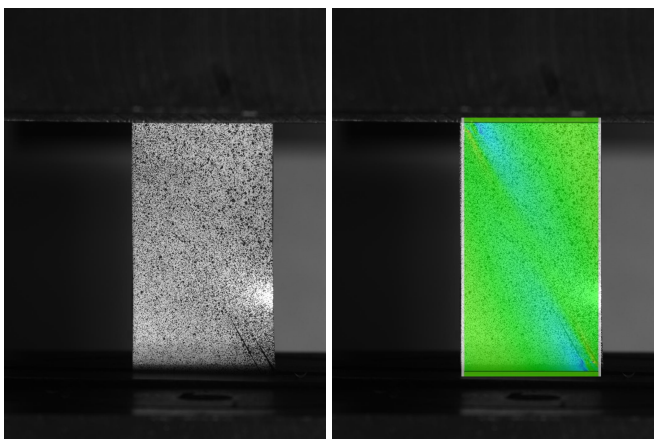

(a) (b)

Figure 9. (a)$[30^o]_{10}$ Off-Axis compression test coupon failure, (b)$[30^o]_{10}$ FEM model x Experimental test final failure.

Also, Fig.9(a) shows the $[30^o]_{10}$ after failure and Fig.9(b) the FEM model superposed the test coupon showing the correspondence between numerical model and experimental test.

7. CONCLUSIONS

This paper proposes an extension to the model by Ladevèze and LeDantec (1992) and Allix *et al.* (1994). The model performs well to predict the behaviour of composite structures for off-axis unidirectional filament winding coupons. The model is implemented as a Fortran subroutine with no need of complex numerical methods (regardless the commercial finite element program).

The simulations were performed with a reasonable computational cost and no convergence problem occur during simulations.

Regarding the model parameters, the experimental tests needed for model parameters possess a reasonable complexity once the necessary equipment and devices are the same used for usual material characterization as tensile and compression tests. Also, the test coupons are easy to manufacture and no special geometry or special manufacture process are required once the manufacture process is the same used for the standard coupons.

8. ACKNOWLEDGEMENTS

The authors are grateful for the financial support from KULeuven Arenberg doctoral school, CAPES and São Paulo Research Foundation (FAPESP process number: 2009/00544-5). The authors also would like to thank CTM for the support.

9. REFERENCES

Allix, O., Ladevèze, P. and Vittecoq, E., 1994. "Modelling and identification of the mechanical behaviour of composite laminates in compression". *Composites Science and Technology*, Vol. 51, No. 1, pp. 35 – 42.

Anderson, T., 1995. *Fracture Mechanics - Fundamentals and Applications*. Second edition edition.

Budiansky, B. and Fleck, N., 1993. "Compressive failure of fibre composites". *Journal of the Mechanics and Physics of Solids*, Vol. 41, No. 1, pp. 183 – 211.

Callister, W.D., 2001. *Fundamentals of Materials Science and Engineering*. John Wiley & Sons, Inc.

Hashin, Z., 1980. "Failure criteria for unidirectional fiber composites". *Journal of Applied Mechanics*, Vol. 47, No. 2, pp. 329–334.

Herakovich, C., 1998. *Mechanics of Fibrous Composites*. first edition edition.

Ladevèze, P. and LeDantec, E., 1992. "Damage modelling of the elementary ply for laminated composites". *Composites Science and Technology*, Vol. 43, No. 3, pp. 257 – 267.

Lapczyk, I. and Hurtado, J.A., 2007. "Progressive damage modeling in fiber-reinforced materials". *Composites Part A: Applied Science and Manufacturing*, Vol. 38, No. 11, pp. 2333 – 2341. CompTest 2006.

Maimí, P., Camanho, P., Mayugo, J. and Dávila, C., 2007. "A continuum damage model for composite laminates: Part i - constitutive model". *Mechanics of Materials*, Vol. 39, No. 10, pp. 897 – 908.

Matzenmiller, A., Lubliner, J. and Taylor, R.L., 1995. "A constitutive model for anisotropic damage in fiber-composites". *Mechanics of Materials*, Vol. 20, No. 2, pp. 125 – 152.

Pinho, S.T., 2005. *Modelling failure of laminated composites using physically-based failure models*. Ph.D. thesis, Imperial College.

Puck, A. and Schürmann, H., 1998. "Failure analysis of frp laminates by means of physically based phenomenological models". *Composites Science and Technology*, Vol. 58, No. 7, pp. 1045–1067.

Puck, A. and Schürmann, H., 2002. "Failure analysis of frp laminates by means of physically based phenomenological models". *Composites Science and Technology*, Vol. 62, No. 12-13, pp. 1633 – 1662.

Tay, T., Liu, G., Tan, S.V., Sun, C.X. and Phan, D., 2008. "Progressive failure analysis of composites". *Journal of Composite Materials*, Vol. 42, pp. 1921 – 1966.

Tita, V., 2003. *Contribuição ao estudo de danos e falhas progressivas em estruturas de material compósito polimérico*. Ph.D. thesis, Escola de Engenharia de São Carlos.

Travessa, A.T., 2006. *Simulation of delamination in composites under quasi-static and fatigue loading using cohesive zone models*. Ph.D. thesis, Universitat de Girona.

Van Der Meer, F. and Sluys, L., 2009. "Continuum models for the analysis of progressive failure in composite laminates". *Journal of Composite Materials*, Vol. 43, No. 20, pp. 2131–2156.

Wisnom, M., 1990. "The effect of fibre misalignment on the compressive strength of unidirectional carbon fibre/epoxy". *Composites*, Vol. 21, No. 5, pp. 403 – 407.

Yokozeki, T., Ogasawara, T. and Ishikawa, T., 2005. "Effects of fiber nonlinear properties on the compressive strength prediction of unidirectional carbon-fiber composites". *Composites Science and Technology*, Vol. 65, No. 14, pp. 2140

– 2147.

10. Responsibility notice

The authors are the only responsible for the printed material included in this paper